journal

Low-Temperature Sintering Li₂MoO₄/Ni₀.₅Zn₀.₅Fe₂O₄ Magneto-Dielectric Composites for High-Frequency Application

Li He,[‡] Di Zhou,[‡] Haibo Yang,[§] Yujuan Niu,[‡] Feng Xiang,[‡] and Hong Wang[‡,†]

[‡]Electronic Materials Research Laboratory, Key Laboratory of the Ministry of Education and International Center for Dielectric Research, Xi'an Jiaotong University, Xi'an 710049, China

[§]School of Materials Science and Engineering, Shaanxi University of Science and Technology, Xi'an 710021, China

The coexistence of Li₂MoO₄ (LMO) and Ni₀.₅Zn₀.₅Fe₂O₄ (NZO) has been proven and their low-temperature-sintered magneto-dielectric composites $(1 - x)$LMO–xNZO (volume fraction factor $x = 0.1, 0.3, 0.5, 0.7$) were prepared by the conventional solid-state reaction method and were sintered below 700°C. It is found that the optimal sample ($x = 0.5$) has good and relatively stable magneto-dielectric performance in the frequency range from 10 MHz to 1 GHz with permittivity between 7.14 and 6.84, dielectric loss tangent between 0.09 and 0.02, and permeability between 5.23 and 3.30, magnetic loss tangent between 0.06 and 0.65, respectively. Furthermore, the verified chemical compatibility with silver indicates that the LMO–NZO ceramics are potential for low-temperature cofired ceramic application and their multifunctional magneto-dielectric properties also make them for potential applications in electronic devices.

I. Introduction

THE magneto-dielectric materials have been widely studied in recent years to meet the requirements of circuit dimension shrinking and high level of passive integration.[1–3] Generally, the polymer-based composite and the multiphase cofired ceramic are the two main important ways which are commonly used in preparation of the magneto-dielectric materials.[4,5]

The composites based on the polymer matrix always have low magnetic and dielectric loss tangents with similar values of permittivities (ε') and permeabilities (μ') within a certain frequency range.[1,2,6–9] These materials with both high inductive and capacitive have been identified to be an enabling solution to fabricate miniature filter and antenna, electromagnetic interference (EMI) devices and so on. However, due to the low melting temperature of the polymer matrix, the derived composites can hardly be used at high-temperature range above 200°C.[10] Compared with the polymer-based composites, the ceramic-based composites always show much higher dielectric and magnetic losses with the permittivities much larger than the permeabilities. Furthermore, most of the reported magneto-dielectric ceramic materials have very high sintering temperature (>900°C), which limits the potential of the materials for the low-temperature cofired ceramic (LTCC) application.[11–16] Therefore, new kinds of low-temperature-sintered magneto-dielectric ceramic with higher values of ε' and μ', and very low magnetic and dielectric loss tangent are desirable.

In the previous studies, dielectric materials with high permittivity and high sintering temperature, which are similar with that of the ferrites, have always been chosen to make the multiphase cofired ceramics together with various kinds of ferrites. Thus, the sintering temperature of the composite ceramics is usually high, because few ferrites can be sintered below 900°C. Meanwhile, these composites always show much larger permittivity than the permeability. Furthermore, during the sintering process, with the grain growth, the increased internal stress between the two phases of dielectric and ferrite can lead to some unusual phase transition or interfacial effect which may cause unpredictable impact on the dielectric and magnetic performance.[17] If an ultralow-temperature-sintered microwave dielectric material can be found to coexist with a ferrite at its own sintering temperature, then a magneto-dielectric ceramic composite with ferrite grains uniformity dispersed into the fully developed dielectric grains can be expected by adjusting the proper proportion of the two phases. This kind of novel composite will have stable and similar permittivity and permeability which seems like the polymer-based composite materials. Meanwhile, the volume fraction upper limit, the heat-deformation temperature will all be largely improved. Furthermore, the very low sintering temperature may be another potential advantage for its LTCC technology application.

In our previous works, an orthorhombic microwave dielectric ceramic Li₂MoO₄ (LMO) with ultralow sintering temperature (540°C) has been reported.[18] Compared with the commonly used polymer substrate materials, such as the Polyvinylidene Fluoride ($\varepsilon' = 6.85$, tan $\delta_\varepsilon = 0.21$ @1 MHz, $\varepsilon' = 2.47$, tan $\delta_\varepsilon = 0.044$ @5 GHz),[19] LMO shows similar permittivity and much lower dielectric loss ($\varepsilon' = 7.14$, tan $\delta_\varepsilon = 0.09$ @1 MHz, $\varepsilon' = 5.5$, tan $\delta_\varepsilon = 2.83 \times 10^{-4}$ @13 GHz). Ni–Zn ferrite is a series of good magnets with very high permeability and very low magnetic loss below the cut-off frequency, and it is often used to produce various of magnetic composites.[20] Here, we have prepared homogeneous cofired ceramic composites by dispersing Ni₀.₅Zn₀.₅Fe₂O₄ (NZO) particles into LMO and sintering them together at low temperature. These results provide a useful approach to fabricate low-temperature-sintered magneto-dielectric ceramic composites and to facilitate their applications in filters, antennas, and EMI device, and other relative fields. The processing route, sintering behavior, microstructures, and dielectric and magnetic properties of the ceramics are presented in details in the following sections.

II. Experimental Procedure

Li₂MoO₄ (LMO) was prepared from reagent-grade LiCO₃ and MoO₃, which were mixed and then calcined at 540°C for 4 h. Ni–Zn ferrite with a composition of NZO was prepared from reagent-grade NiO, ZnO, and Fe₂O₃, which were mixed and then calcined at 1000°C for 4 h. All the starting materi-

---

als were from Sinopharm Chemical Reagent, Shanghai, China and their purities are higher than 99%. According to different mass ratio, LMO powder and NZO powder were mixed together and remilled in ethanol with ZrO_2 as the milling media using a planetary mill (Nanjing Machine Factory, Nanjing, China), and then the obtained final powder mixtures were pressed into disks and rings after adding 5 wt% polyvinyl alcohol. Final sintering was carried out at 650°C–690°C in air for 2 h. It was found that the densities of the ceramic composite increased with the increasing of the sintering temperature, however, the samples began to melt at above 690°C. Therefore, the sintering temperature of all the samples in this experiment was set to 685°C. To study the chemical compatibility with Ag, ceramic samples were ground and mixed into composites with 20 wt% Ag powders, and then sintered at around 680°C for 2 h.

The crystalline structures of samples were investigated using X-ray diffraction with CuK_α radiation (RigakuD/MAX-2400X-ray diffractometer, Tokyo, Japan). Microstructures of the sintered ceramics were observed on the fracture surfaces with scanning electron microscopy (SEM) (Quatan250FEG; FEI, Hillsboro). The DC resistivities of the ceramics were measured by a high-resistance meter (4339, Hewlett Packard, Palo Alto, CA) with a component test fixture (16339A) at room temperature. The dielectric properties of the ceramic in the low-frequency range (100 Hz–1 MHz) were measured by an impedance analyzer (4980, Agilent, Palo Alto, CA). The dielectric and magnetic measurements in higher frequency range (1 MHz–1 GHz) were carried out by an impedance analyzer (4291B, Hewlett Packard, Palo Alto, CA) with a dielectric material test fixture (16453A) and magnetic material test fixture (16454L), respectively. The magnetic hysteresis loops of the composites were measured by a vibrating sample magnetometer (VSM-7307; Lake Shore, Westerville, OH).

III. Results and Discussion

The XRD pattern in Fig. 1 shows the LMO–NZO ceramic with 50% NZO concentration sintered at 685°C. It can be seen that in the composite there is no any other phase being detected besides the main phases of LMO and NZO, indicating that the two phases can exist individually and display very good chemical compatibility at 685°C. Figure 1 contains the SEM micrographs of the LMO–NZO composites with different NZO concentration, and the two phases can be distinguished clearly by the different particle size. After the ball mill mixing process, the particle size of both LMO and NZO starting powders is about 1 μm. For the sintering temperature is higher than that of the LMO (540°C)[18] but much lower than that of the NZO (1300°C),[20] the NZO particle size is little-changed in each composition, whereas the grain size of LMO is significantly increased (about 20 μm when $x = 0.1$ @685°C) during the sintering process. Furthermore, the more NZO a sample contains the smaller LMO grain size it shows, because the NZO grains absorb more heat and they separate and limit the growth of the LMO grains during the sintering process. The microstructures of the composites exhibit apparent concrete-like morphologies with the uniformly distributed individual smaller NZO particles being surrounded by lager LMO matrix.

Figure 1 also presents the bulk densities and the relative densities of the LMO–NZO ceramics sintered at 685°C as a function of the volume fraction factor x. The sintered pure LMO ceramic has a bulk density of 2.895 g/cm^3 and a relative density of 95.5% at 540°C. With the increasing of x value, the bulk density of the LMO–NZO ceramic increased because the NZO has larger bulk density of 5.3 g/cm^3. However, the relative density decreased comparing with the calculated theoretical density because the increase content of NZO particles disturbed the interaction between each developing LMO grains as mentioned before. Therefore, with the increasing of x value, the LMO grains become smaller and the relative density also decreases which are in consistent with the experimental results. In other words, the excessive NZO will lead to a decrease densification of the composite ceramics. It can be seen that the densities of composites are all more than 90% ($x \leq 0.5$), indicating that these composite ceramics are dense and well sintered at this temperature.

Figure 2 shows the frequency dependence of permittivity and dielectric loss of the composites with different NZO concentration in a very wide frequency range from 100 Hz to 1 GHz. For each component, the relative permittivity and dielectric loss are very high in low test frequency range. They decrease with the increasing of test frequency and finally become almost constant in higher frequency range (>10 MHz).

At lower frequency, the permittivities of the composites are very high and the frequency dispersion of permittivities is
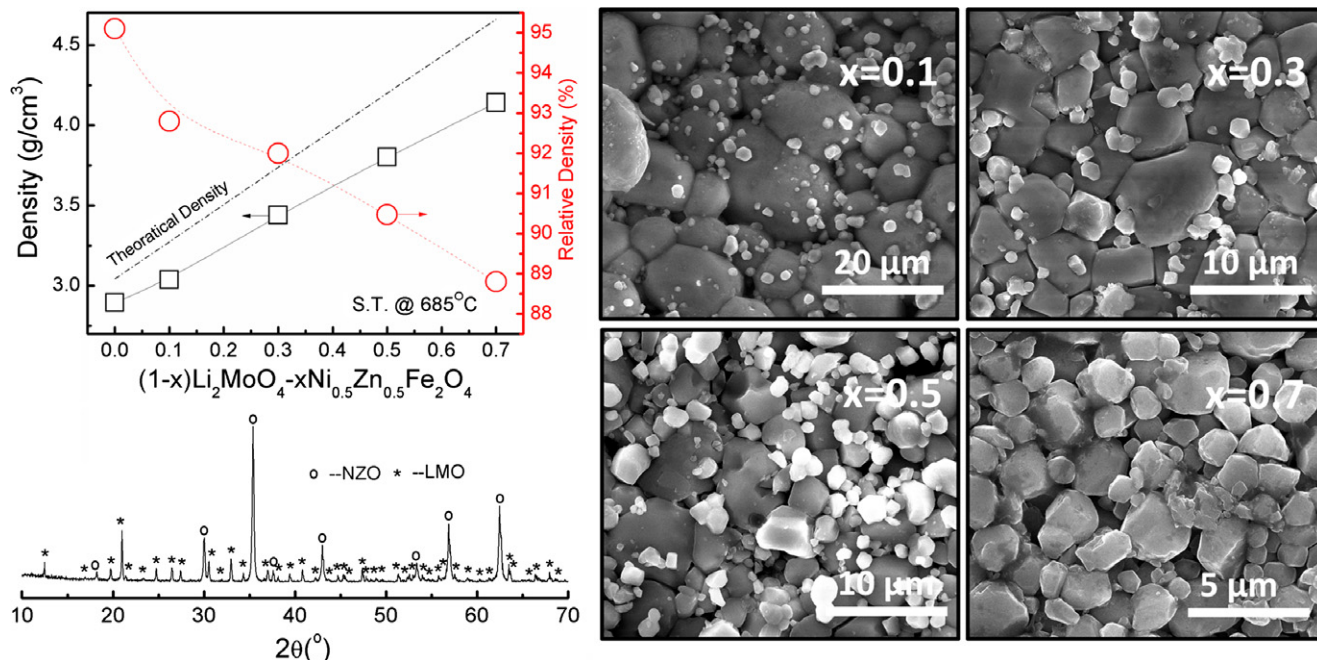

Fig. 1. The bulk densities and the relative densities, the calcined XRD patterns and the 685°C sintered SEM micrographs of the $(1-x)$LMO–xNZO ceramics.
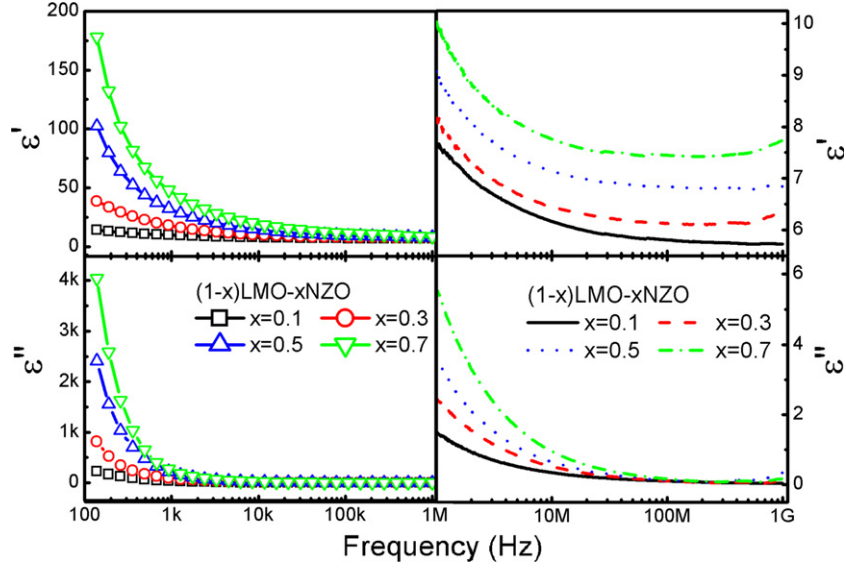
Fig. 2. The frequency dependency of dielectric properties of the $(1-x)$LMO–xNZO ceramics in wide frequency range from 100 Hz to 1 GHz.
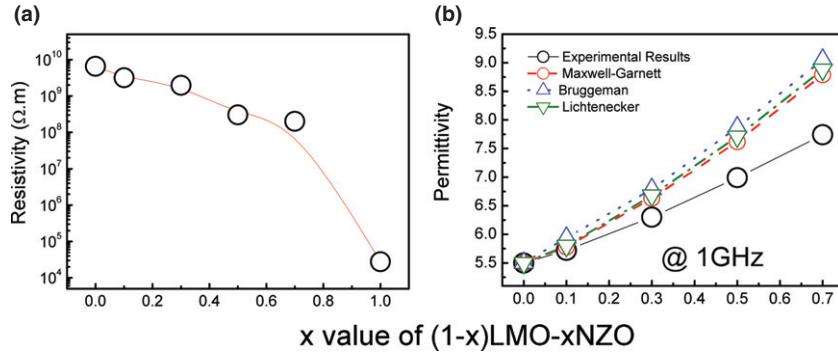

Fig. 3. (a) The room-temperature DC electrical resistivity and (b) the experimental data and calculated permittivities of the $(1-x)$LMO–xNZO ceramics.

stronger with the increase in the NZO concentration. With frequency increasing, the permittivities are becoming smaller and not very sensitive to the NZO concentration as that observed at lower frequencies. According to the two-layer model of Maxwell–Wagner interfacial polarization,[21] the space charge polarization arises in the inhomogeneous structure dielectric materials. The NZO grains with relatively higher conductivity are dispersed in the higher resistive LMO substances. This causes the localized accumulation of charges under the influence of electric field, which results in the interfacial polarization and seriously influenced the low-frequency permittivities. At higher frequencies, the interfacial polarization cannot follow the quickly alternating field, which causes an obvious decrease of the permittivity. Therefore, a decrease in permittivity can be observed with the frequency increasing.

The dielectric loss always can be described by the following Debye formula:[12]

$$D = D_P + D_G = \frac{(\varepsilon_S - \varepsilon_\infty)\omega\tau}{\varepsilon_S + \varepsilon_\infty\omega^2\tau^2} + \frac{\gamma}{\omega\varepsilon_0}\frac{1}{\varepsilon_\infty + \frac{\varepsilon_S-\varepsilon_\infty}{1+\omega^2\tau^2}}, \quad (1)$$

where D is the total dielectric loss, D_P is the polarization loss and D_G is the leakage loss, τ and γ refer to the relaxation time and the conductivity, whereas the ε_0 and ε_∞ denote the relative permittivity of state electrical field and optical frequency, respectively. When the test frequency is very low $(\omega\to0)$, the polarization loss D_P is close to zero, and in this case, the dielectric loss which almost attributed to the leakage loss and can be approximately described as

$$D \cong \frac{\gamma}{\omega\varepsilon_0\varepsilon_S}. \quad (2)$$

Thus, the dielectric loss is inversely proportional to the test frequency in the low-frequency range. Furthermore, according to the expression (2), the low-frequency dielectric loss will also be seriously influenced by the conductivity of the materials. Figure 3(a) shows the room-temperature DC electrical resistivity as a function of the x value. With the increase in the x value, the DC resistivity of the ceramics presents an exponential decrease, which can be attributed to the continuous increase in higher conductivity NZO particles. This result can be used to explain the rapidly increasing of dielectric loss with x value in the low-frequency range.

The Maxwell–Garnett (MG) rule [Eq. (3)], the Bruggeman rule [Eq. (4)], and the Lichtenecker logarithmic rule [Eq. (5)], are all the classical mixing rules to predict the effective permittivity of a two-phase mixture.[22,23]

$$\varepsilon_{\text{eff}} = \varepsilon_2 + 3v_2\varepsilon_2 \frac{\varepsilon_1 - \varepsilon_2}{\varepsilon_1 + 2\varepsilon_2 - v_2(\varepsilon_1 - \varepsilon_2)} \quad (3)$$

$$v_1\frac{\varepsilon_1 - \varepsilon_{\text{eff}}}{\varepsilon_1 + 2\varepsilon_{\text{eff}}} + v_2\frac{\varepsilon_2 - \varepsilon_{\text{eff}}}{\varepsilon_2 + 2\varepsilon_{\text{eff}}} = 0 \quad (4)$$

$$\lg\varepsilon_{\text{eff}} = v_1 \times \lg\varepsilon_1 + v_2 \times \lg\varepsilon_2 \quad (5)$$

where ε_{eff}, ε_1, and ε_2 are the effective permittivities of the composite and the two different dielectric materials, and v_1

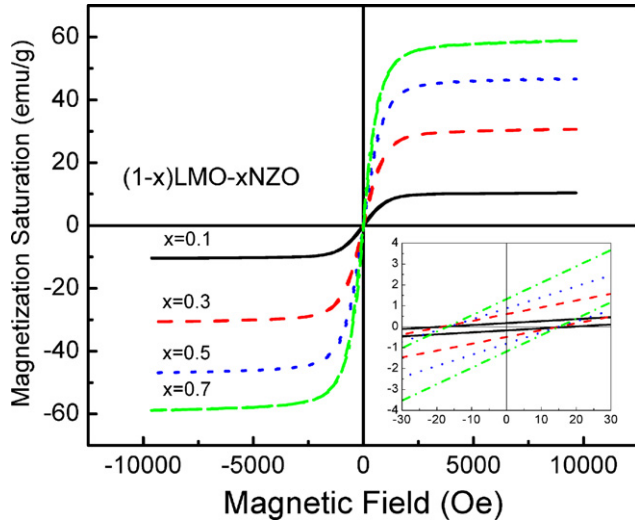**Fig. 4.** The magnetic hysteresis loops of the $(1-x)$LMO–xNZO ceramics in the magnetic field range of $-10\,000$ to $10\,000$ Oe and -30 to 30 Oe.

Fig. 6. The backscattered electron images and the XRD patterns of the 0.5LMO–0.5NZO + 20 wt% Ag sintered at 680°C for 2 h.

and v_2 are the volume fractions of the corresponding materials ($v_1 + v_2 = 1$), respectively.

In this study, the calculated results obtained by these models are used to compare with the measured results as shown in Fig. 3(b). The differences between the three calculated results are due to the different applications cope of these models. Generally, the MG rule is commonly used in composites with a small amount of fillers randomly dispersed into a host material. The Bruggeman rule is applied in compounds where two randomly distributed phases have similar morphologies. While the Lichtenecker formula is an empirical rule, which is suitable for composite materials aligned randomly. When the content of NZO is low, the measured results fit well with the model curves. However, with the increase in x value, the composite materials show smaller permittivity than the calculated value. That is mainly due to the gradually decreasing densification, as shown in Fig. 1, which caused the decrease of the composite permittivity in higher filler concentration.

Figure 4 shows the magnetic hysteresis loops of the $(1-x)$ LMO–xNZO composites with different x value. It can be seen that the saturation magnetization (M_S) and the remnant magnetization (M_r) increase with the increasing of the NZO content, as expected, because these parameters depend on the total mass of the magnetic material. The reduction of the M_S values is mainly due to the dilution of the magnetic component.[24] The coercivity (H_c) always keeps constant with the variation of NZO content, which indicates that the NZO grains in all the samples have very similar microstructure and surface morphology.[10]

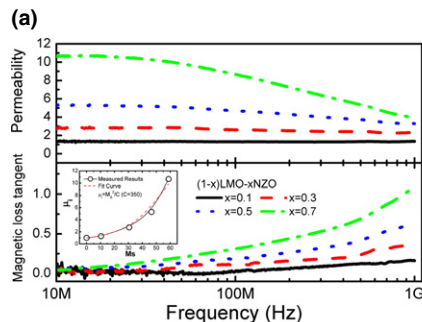The frequency dependence of the magnetic properties of the $(1-x)$LMO–xNZO composite with different x value is

shown in Fig. 5(a). It can be seen that the initial permeability and magnetic loss of the composite increase with x value increasing. Meanwhile, when the NZO content is not more than 50%, each curve shows good frequency stability and relatively low magnetic loss within 1 GHz.

It is well-known that the initial permeability (μ_i) of ferrite is strongly affected by M_S, crystal magnetization anisotropy (K_1), magnetostriction constant (λ_S), and internal stress (σ), and thus it can be expressed as in the following equation:

$$\mu_i = M_S^2/(aK_1 + b\lambda_S\sigma), \qquad (6)$$

a and b are constants.[25] In the LMO–NZO composites, as mentioned before, the NZO grains have very similar microstructure and surface morphology, thus the K_1, λ_S, and σ will have little impact on the initial permeability and can be all regarded as constants. Accordingly, the Eq. (6) can be simplified as

$$\mu_i = M_S^2/C, \qquad (7)$$

which fits well with the measured results ($C = 350$) as the inset shown in Fig. 5(a). Furthermore, according to the Snoek's law,[26] the product of the initial susceptibility and resonance frequency is constant for ferromagnetic material, that is, $(\mu_i-1) \times f_r = \gamma/2\pi M_S$, where f_r is the cut-off frequency, and γ is the gyromagnetic ratio. The increase in the NZO concentration will cause the increase of M_S as well as μ_i, thus a decreasing cut-off frequency with the increasing NZO concentration can also be expected.

Fig. 5. (a) The frequency dependency of magnetic properties of the $(1-x)$LMO–xNZO ceramics in the frequency range of 10 MHz–1 GHz, and (b) Curve fitting of the dependence of effective permeability(μ') on volume fraction (p) and demagnetizing factor (N_d), based on the Maxwell–Garnett mixing law, respectively.
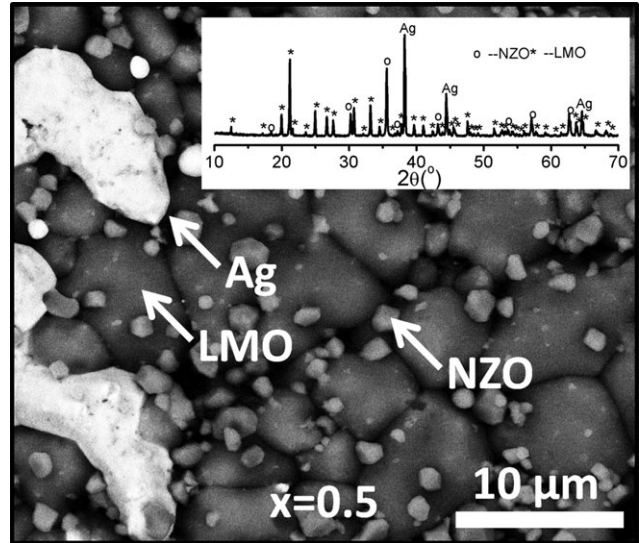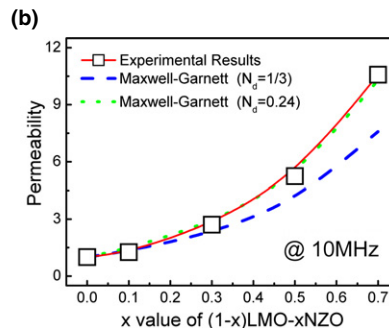
For illustration and comparison, the theoretical calculations of the permeabilities using the well-known MG mixing law:

$$\mu_{eff} = \frac{(\mu_i - 1)p}{(\mu_i - 1)(1 - p)N_d + 1} + 1 \tag{8}$$

where N_d is the demagnetizing factor of the fillers, p is the volume fraction, and μ_i is the initial permeability of the bulk magnetic materials.[27,28] For the two-phase composite of spherical ferrites and nonmagnetic host matrix, the demagnetizing factor N_d is equal to 1/3, and the calculated data is shown by the blue-dash curve in Fig. 5(b). However, the measured results are a little higher than the calculations. It can be seen in the SEM micrographs that the calcined NZO grains are not precisely spherical, but composed of angular grains with rough surfaces. Therefore, compared with the regular spherical fillers, the angular NZO grains are likely to cause the change in the aspect ratio as well as the demagnetizing factor N_d. The calculated curve with N_d equals to 0.24 fits well with the experiment results which indicates the NZO grains have smaller aspect ratio than the ideal spherical magnetic fillers.

For the LMO and NZO ceramics, they have already been proven to not react with silver, respectively, the chemically compatible with Ag of their composite can also be expected. Figure 6 presents the XRD patterns and backscattered electron image of 0.5LMO–0.5NZO composite ceramic cofired with Ag at 680°C for 2 h. Both the XRD patterns and the back scattered electron image analysis reveal that the reaction of low-fired LMO–NZO ceramics with Ag electrodes did not occur. And therefore, the cofiring of LMO–NZO ceramics with silver electrodes is feasible.

IV. Conclusions

Ceramics of LMO and NZO differing widely in the sintering temperature are proved to be sintered together at 685°C without any chemical reaction in between. Therefore, the low-temperature sintering and the good dielectric properties of the microwave dielectric materials LMO as well as the good magnetic properties of the ferrite NZO can be integrated together into a multifunctional material of $(1-x)$LMO–xNZO composite ceramics. The samples ($x \leq 0.5$) possess both good and stable magneto-dielectric properties in the frequency range from 10 MHz to 1 GHz with acceptable good densities. In this study, a novel design thought of selecting low-temperature sintering microwave dielectric ceramic as matrix are put forward. Compared with the polymer-based composites, the heat-deformation temperature of the ceramic-based composite material is significantly increased. Meanwhile, the volume fraction upper limit and the comprehensive magneto-dielectric properties have been improved. Furthermore, the chemically compatibility of the 680°C sintered ceramic with silver has also been verified. The LMO–NZO composite ceramics with stable magneto-dielectric properties for integrated electronics are a kind of suitable candidates for the low-temperature cofired ceramic technology application.

References

[1]L. B. Kong, Z. W. Li, G. Q. Lin, and Y. B. Gan, "Ni-Zn Ferrites Composites with Almost Equal Values of Permeability and Permittivity for Low-Frequency Antenna Design," *IEEE Trans. Magn.*, **43** [1] 6–10 (2007).

[2]H. B. Yang, H. Wang, F. Xiang, and X. Yao, "Multifunctional SrTiO₃/NiZn Ferrite/POE Composites With Eletromagnetic and Flexible Properties for RF Applications," *J. Electroceram.*, **22** [1–3] 221–6 (2009).

[3]A. Thakur, A. Chevalier, J. L. Mattei, and P. Queffelec, "Low-Loss Spinel Nanoferrite With Matching Permeability and Permittivity in the Ultrahigh Frequency Range," *J. Appl. Phys.*, **108** [1] 014301, 4pp (2010).

[4]H. Wang, H. B. Yang, F. Xing, and X. Yao, "Low-Loss Electromagnetic Composites for RF and Microwave Applications," *IEEE Trans. Ultrason. Ferroelectr. Freq. Control*, **58** [9] 1947–53 (2011).

[5]J. Ma, J. Hu, Z. Li, and C.-W. Nan, "Recent Progress in Multiferroic Magnetoelectric Composites: From Bulk to Thin Films," *Adv. Mater.*, **23** [9] 1062–87 (2011).

[6]L. J. Martin, S. Ooi, D. Staiculescu, M. D. Hill, C. P. Wong, and M. M. Tentzeris, "Effect of Permittivity and Permeability of a Flexible Magnetic Composite Material on the Performance and Miniaturization Capability of Planar Antennas for RFID and Wearable Wireless Applications," *IEEE Trans. Compon. Packag. Technol.*, **32** [4] 849–58 (2009).

[7]J. Jeong Keun, A. Won Ki, K. Jun Sig, P. Sang Hoon, K. Gi Ho, and S. Won Mo, "Miniaturized T-DMB Antenna With a low-Loss Ni-Mn-Co Ferrite for Mobile Handset Applications," *IEEE Magn. Lett.*, **1**, 5000104, 4pp (2010).

[8]D. Souriou, J. L. Mattei, A. Chevalier, and P. Queffelec, "Influential Parameters on Electromagnetic Properties of Nickel-Zinc Ferrites for Antenna Miniaturization," *J. Appl. Phys.*, **107** [9] 09A518, 3pp (2010).

[9]M. Teirikangas, J. Juuti, and H. Jantunen, "Layered Dielectric-Magnetic Composite Structures for Rf-Applications," *Compos. Struct.*, **93** [1] 179–83 (2010).

[10]L. He, H. B. Yang, D. Zhou, Y. J. Niu, F. Xiang, and H. Wang, "Improved Dielectric and Magnetic Properties of 1-3-Type Ni₀.₅Zn₀.₅Fe₂O₄/Epoxy Composites for High-Frequency Applications," *J. Phys. D: Appl. Phys.*, **46**, 125003, 7pp (2013).

[11]H. I. Hsiang and T. H. Chen, "Dielectric and Magnetic Properties of Low-Temperature-Fired Ferrite-Dielectric Composites," *J. Am. Ceram. Soc.*, **91** [6] 2043–6 (2008).

[12]H. B. Yang, H. Wang, F. Xiang, and X. Yao, "Microstructure and Electromagnetic Properties of SrTiO₃/Ni₀.₈Zn₀.₂Fe₂O₄ Composites by Hybrid Process," *J. Am. Ceram. Soc.*, **92** [9] 2005–10 (2009).

[13]L. P. Curecheriu, M. T. Buscaglia, V. Buscaglia, L. Mitoseriu, P. Postolache, A. Ianculescu, and P. Nanni, "Functional Properties of BaTiO₃–Ni₀.₅Zn₀.₅Fe₂O₄ Magnetoelectric Ceramics Prepared From Powders with Core-Shell Structure," *J. Appl. Phys.*, **107** [10] 104106, 11pp (2010).

[14]Z. Zheng and H. Zhang, "Complex Permittivity and Permeability of Low-Temperature Sintered M-Type Barium Hexaferrite in Ka-Band Frequency Range," *IEEE Trans. Magn.*, **49** [7] 4230–3 (2013).

[15]H. F. Zhang, S. W. Or, and H. L. W. Chan, "Fine-Grained Multiferroic BaTiO₃/(Ni₀.₅Zn₀.₅)Fe₂O₄ Composite Ceramics Synthesized by Novel Powder-in-sol Precursor Hybrid Processing Route," *Mater. Res. Bull.*, **44** [6] 1339–46 (2009).

[16]J. Lee, Y. K. Hong, S. Bae, J. Jalli, G. S. Abo, J. Park, W. M. Seong, S. H. Park, and W. K. Ahn, "Low Loss Co₂Z (Ba₃Co₂Fe₂₄O₄₁)-Glass Composite for Gigahertz Antenna Application," *J. Appl. Phys.*, **109** [7] 07E530, 4pp (2011).

[17]H. B. Yang, H. Wang, L. He, L. Shui, and X. Yao, "Polarization Relaxation Mechanism of Ba₀.₆Sr₀.₄TiO₃/Ni₀.₈Zn₀.₂Fe₂O₄ Composite With Giant Dielectric Constant and High Permeability," *J. Appl. Phys.*, **108** [7] 074105, 4pp (2010).

[18]D. Zhou, C. A. Randall, H. Wang, L. X. Pang, and X. Yao, "Microwave Dielectric Ceramics in Li₂O–Bi₂O₃–MoO₃ System with Ultra-Low Sintering Temperatures," *J. Am. Ceram. Soc.*, **93** [4] 1096–1100 (2010).

[19]K. Yu, Y. Niu, Y. Zhou, Y. Bai, and H. Wang, "Nanocomposites of Surface-Modified BaTiO₃ Nanoparticles Filled Ferroelectric Polymer with Enhanced Energy Density," *J. Am. Ceram. Soc.*, **96** [8] 2519–24 (2013).

[20]A. Costa, E. Tortella, M. R. Morelli, and R. Kiminami, "Synthesis, Microstructure and Magnetic Properties of Ni–Zn Ferrites," *J. Magn. Magn. Mater.*, **256** [1–3] 174–82 (2003).

[21]I. H. Gul, F. Amin, A. Z. Abbasi, M. Anis-ur-Rehmanb, and A. Maqsood, "Physical and Magnetic Characterization of co-Precipitated Nanosize Co-Ni Ferrites," *Scripta Mater.*, **56** [6] 497–500 (2007).

[22]F. Brouers, "Percolation Threshold and Conductivity in Metal-Insulator Composite Mean-Field Theories," *J. Phys. C: Solid State Phys.*, **19** [36] 7183–93 (1986).

[23]R. Simpkin, "Derivation of Lichtenecker's Logarithmic Mixture Formula from Maxwell's Equations," *IEEE Trans. Microw. Theory*, **58** [3] 545–50 (2010).

[24]S. L. Young, H. Z. Chen, C. C. Lin, J. B. Shi, L. Horng, and Y. T. Shih, "Magnetotransport Properties of (La₀.₇Pb₀.₃MnO₃)₍₁₋ₓ₎–Agₓ Composites," *J. Magn. Magn. Mater.*, **303** [2] E325–8 (2006).

[25]M. Fujimoto, K. Hoshi, M. Nakazawa, and S. Sekiguchi, "Cu Multiply Twinnned Particle-Precipitation in low-Temperature Fired Ni–Zn–Cu Ferrite," *Jpn. J. Appl. Phys.*, **32** [12A] 5532–6 (1993).

[26]L. Snoek, "New Developments in Ferromagnetic Materials," *Physica (Amsterdam)*, **14**, 207–17 (1948).

[27]Z. W. Li, Z. H. Yang, and L. B. Kong, "Enhanced Microwave Magnetic and Attenuation Properties for Z-Type Barium Ferrite Composites with Flaky Fillers," *J. Appl. Phys.*, **110** [6] 063907, 7pp (2011).

[28]Z. W. Li, Y. B. Gan, X. Xin, and G. Q. Lin, "Characteristics of Effective Permeability and Resonance Frequency for Barium-Ferrite/Epoxy Composites," *J. Appl. Phys.*, **103** [7] 073901, 8pp (2008). □